

TREND SURFACE ANALYSIS AND SPLINES FOR PATTERN DETERMINATION IN PLANT COMMUNITIES

Ladislav Mucina, Department of Geobotany, Institute of Experimental Biology and Ecology S.A.S., Sienkiewiczova 1, CS-814 34 Bratislava, Czechoslovakia, Present (and corresponding) address: Department of Vegetation Ecology and Nature Conservancy, Institute of Plant Physiology, University of Vienna, Althanstrasse 13, A-1091 Wien, Austria
Viliam Čik, Institute of Mathematics and Computing Machinery, Comenius University, Šafárikovo nám. 6, CS-818 06 Bratislava, Czechoslovakia
and Peter Slavkovský, Computer Centre of the Slovak Academy of Sciences, Dúbravská cesta 9, CS-842 35 Bratislava, Czechoslovakia

Keywords: Approximation, Bicubic splines, Computer graphics, Goodness of fit, Interpolation, Trend surface analysis, Triangular splines, Vegetation pattern

Abstract: Some approximation and interpolation approaches to mapping ecological and vegetation variables on a surface are presented. In this connection trend surface analysis based on polynomial regression is shown to be a promising technique. It is reviewed and typical applications are presented. Basic features of the mathematical background for bicubic and triangular splines are discussed. 'Splines' is a family of powerful interpolation techniques for mapping of ecological and vegetational variables both on regular and irregular grids.

1. General Introduction

Searching for pattern in vegetation occupies a large field in vegetation science, and is considered one of many current studies. While different simple and sophisticated pattern techniques were developed or introduced into vegetation studies, mainly the techniques designed for searching for area-based patterns are gaining in importance.

Vegetation can be seen as a result of both co-operation and antagonistic actions of various ecological factors, including population interactions which operate either on general or on local scales. Separation of the general and local factors is a complex task and calls for an adequate pattern analysis methods. A family of methods, termed trend surface analysis (further TSA), is one of those. TSA allows separation of the global trends from local deviations assumed to be a response to local factors. Trend is understood as the systematic pattern of variation inherent in the data, or a mathematical function describing that pattern.

Another group of mapping methods is based on polynomial splines. The polynomial splines are a tool for studying local factors in a site. Unlike TSA, the coefficients of splines depend on measured values only in a limited surrounding of the considered subregion. While TSA is an approximation method, splines belong to interpolation methods.

Both TSA and splines techniques have a number of characters in common. In ecological context, they are adopted as tools for pattern inference both of single-variable as well as multivariable patterns. The keywords of this chapter are the approximation and interpolation, concepts bearing on pattern recognition (inference) and its representation.

Vegetation and ecological data, if measured in a

particular region, can be graphically depicted in maps. TSA and splines provide a tool for quantitative vegetation mapping.

2. Trend Surface Analysis

2.1. Introduction

Trend surface analysis is a family of methods aimed to describe spatial patterns in mapped data or temporal trends in time-series data possessing a relation to mapped surface. The patterns are supposed to vary systematically over the mapped area. The difference between the systematic trend and raw data produce residuals for each of the measured points. The residuals are interpreted in terms of regional factors operating at a local scale and producing regional trends. The method generalizes the spatial distribution of dependant variables in Euclidean space by means of a corresponding function. Cover values of species in samples, soil characteristics and the like might be the dependant variables, coordinates of the samples in an area are the independent variables, and polynomial regression is the corresponding function. TSA is based on the construction of polynomials by the least-square method, which minimalizes the sum of squares between the measured values and the fitted surface (Grant 1957, Krumbein 1959, Gittins 1968, Norcliffe 1969, Watson 1971, Unwin 1975, Goodman 1983a).

Early biological applications of the polynomial TSA were made in biogeography (Stehli and Helsley 1963, Sokal and Rinkel 1963, Stehli 1964, 1965, Stehli and Welles 1971, Durazzi and Stehli 1972). Later, it was found to be useful in taxonomy and morphometrics (Sneath 1967, Sokal and Ogden 1978, see also Sneath and Sokal 1973), and palynology (McAndrews and

Power 1973).

Community ecology has profited from the TSA applications only in few papers despite a promising nature of the technique (Fischer 1968, Jumars et al. 1977, Jumars 1978, Hengeveld 1979, Kooijman and Hengeveld 1979). The history of use of TSA in vegetation science is also very brief. The method was used in micro- and meso-scale pattern analysis (Gittins 1968, Mucina and Poláček 1982), aided interpretation of ordinations (Neal and Kershaw 1973, Dargie 1984), and assisted searching for relations in a vegetation structure studies (Curtis and Bignal 1985).

Bonham (1971, see also Reader and Lieth 1984) used orthogonal polynomials for a demonstration of mapping of *Bouteloua chondrosioides*, a prairie plant.

2.2. Polynomial trend surface analysis

Polynomial TSA is based on multiple regression. Spatial coordinates of samples are considered independent variables. The method generalizes the spatial distribution of dependant variables (e.g. cover values of species, or values for soil properties over the study area) in Euclidean space by means of a corresponding trend function.

The separation of surface trends is based on the following additive model:

$$Z_i = f(U_i, V_i) + \epsilon \quad (1)$$

Z_i symbolizes the value of the dependant variable at a point in space determined by coordinates U_i and V_i , $f(U_i, V_i)$ stands for the trend function, and ϵ is the residual (random) component.

The simplest trend function is linear:

$$Y = A_{(0)} + A_{(1)} U + A_{(2)} V + \dots \quad (2)$$

The polynomial coefficients $A_{(0)}$, $A_{(1)}$, $A_{(2)}$, ... can be conceived as regression coefficients (Unwin 1975). More details on the interpretation of coefficients are found in, for instance, Unwin (1975), Haggett et al. (1977), and Goodman (1983b).

The second-order polynomial surface is terminated by 6 coefficients, the third-order one by 10, and the n th order by

$$D = \frac{(n+1) * (n+2)}{2}$$

coefficients, such that

$$Y = A_{(0)} + A_{(1)} U + A_{(2)} V + A_{(3)} U^2 + \dots + A_{(D)} V^n \quad (3)$$

Calculation of trend coefficients. As in regression analysis we apply the least-square method:

$$\sum_{i=1}^p E_i^2 = \sum (Y(U_i, V_i) - Z_i)^2 = \min \quad (4)$$

where p is the number of sample points. The following partial derivatives are set equal to zero:

$$d \sum E_i^2 / d A_0, d \sum E_i^2 / d A_1, \dots, d \sum E_i^2 / d A_D \quad (5)$$

In this way, a system of D normal equations is obtained:

$$\begin{aligned} A_0 * p + A_1 * \sum_{i=1}^p U_i + A_2 * \sum V_i + \dots + A_D * \sum V_i^n &= \sum Z_i \\ A_0 * \sum U_i + A_1 * \sum U_i^2 + A_2 * \sum U_i V_i + \dots + A_D * \sum U_i V_i^n &= \sum U_i Z_i \\ A_0 * \sum V_i^n + A_1 * \sum V_i^n U_i + A_2 * \sum V_i^{n+1} + \dots + A_D * \sum V_i^{2n} &= \sum V_i^n Z_i \end{aligned} \quad (6)$$

The matrix form of the system of equations is:

$$\begin{bmatrix} p & \sum U_i & \sum V_i & \dots & \sum V_i^n \\ \sum U_i & \sum U_i^2 & \sum U_i V_i & \dots & \sum V_i^n U_i \\ \vdots & \vdots & \vdots & \ddots & \vdots \\ \sum V_i^n & \sum U_i V_i^n & \sum V_i^{n+1} & \dots & \sum V_i^{2n} \end{bmatrix} * \begin{bmatrix} A_0 \\ A_1 \\ \vdots \\ A_D \end{bmatrix} = \begin{bmatrix} \sum Z_i \\ \sum U_i Z_i \\ \vdots \\ \sum V_i^n Z_i \end{bmatrix} \quad (7)$$

$$\mathbf{X} * \mathbf{A} = \mathbf{Z} \quad (8)$$

where \mathbf{X} is the cross-products matrix, \mathbf{A} is the coefficients vector, and \mathbf{Z} is the scaled observations vector.

Solving for \mathbf{A} :

$$\mathbf{A} = \mathbf{Z} * \mathbf{X}^{-1} \quad (9)$$

Test for goodness of fit. By definition,

$$\begin{aligned} f_1 &= \sum U_i, f_2 = \sum V_i, f_3 = \sum U_i^2, \dots, \\ f_D &= \sum V_i^n \end{aligned} \quad (10)$$

the total variance is:

$$V_{\text{SUM}} = \sum_{i=1}^p (Z_i - \sum_{j=1}^D (f_j / p))^2 \quad (11)$$

and the variance of the trend function is:

$$V_{\text{TREND}} = \sum_{i=1}^p (f(U_i, V_i) - \sum_{j=1}^D (f_j / p))^2 \quad (12)$$

The coefficient of multiple determination is

$$D = V_{\text{TREND}} / V_{\text{SUM}} \quad (13)$$

2.3. Comparison of trend surface patterns

Having at least two TSA patterns (images) we are interested to measure their similarity. This is a very complex task of many facets, amounting to

- (1) point correlation comparisons;
- (2) coefficient and vector comparisons; and
- (3) surface slope comparisons.

By *point correlation comparisons* Goodman (1983a, b) means the use of structural correlation coefficient of Mirchink and Bukhartsev (1954). This produces a single scalar value, based on differences between comparable points on two surface standartized to a common scale. The coefficient is:

$$r_0 = \frac{\sum_{i=1}^p (\hat{Z}_{1j} - \bar{Z}_1) * (\hat{Z}_{2i} - \bar{Z}_2)}{p S_{z1} S_{z2}} \quad (14)$$

where \hat{Z}_{1j} and \hat{Z}_{2i} are the heights of the two surfaces at a point, \bar{Z}_1 and \bar{Z}_2 are the mean heights, S_{z1} and S_{z2} are the standard deviations, and p is the number of sample points.

The interpretation of low or and upper limits is similar to that of the product-moment correlation coefficient. However, Goodman (1983a) warns against interpretation of a high correlation in the presence of low goodness of fit values. It is relevant that the TSA coefficients vector describes the from of the surface. The base coefficient (A_0) is a measure of absolute height at the origin, while the remaining coefficients describe properties such as shape, orientation, and convexity (Goodman 1983a). Davis (1973) suggested to compare the vectors numerically based on the correlation coefficient,

$$r = \frac{\text{cov}(A_{(i)1}, A_{(i)2})}{\sqrt{(\text{var } A_{(i)1}) * (\text{var } A_{(i)2})}}, \text{ for } i = 1, \dots, D \quad (15)$$

where $A_{(i)1}$ and $A_{(i)2}$ are the coefficient vectors.

Another facet of the TSA pattern comparisons is the *comparison of surface slopes*. Two surface properties, such as slope (dip) and orientation (strike) seem promising in this respect. The simplest form of derivation of values for slope and orientation is that for linear surface. Robinson and Caroe (1967, p. 263-265) compute orientation and slope as follows:

$$\tan \alpha = \frac{A_0}{A_1} \quad (16)$$

$$\Theta = A_0^2 - A_1^2 \quad (17)$$

where A_0 and A_1 are the polynomial coefficients under comparison. Comparison is then quantified using

$$DC_{\text{orientation}} = \cos |\alpha_1 - \alpha_2| \quad (18)$$

$$DC_{\text{slope}} = \cos |\Theta_1 - \Theta_2| \quad (19)$$

$DC_{\text{orientation}}$ and DC_{slope} range from 0 to 1 from perfect correspondence to orthogonality, i.e. perfect dissimilarity. Sneath (1966, see also Goodman 1983a, b) derive measures for comparisons for high-order surfaces.

2.4. Canonical trend surface analysis

Canonical trend surface analysis (CTS) combines the advantages of canonical correlation analysis (CCA; Hotelling 1936, Morrison 1976, Green 1978, Gittins 1979) and TSA. CTS computes multivariate trend surfaces from two variance/covariance matrices in such a way that the correlation is maximized between the linear composite values for the trend surfaces and linear composite values for the set of variables. One of the variance/covariance matrices is based on geographical coordinates for sampled points and the other derived from a set of multivariate observations at locations identified by the geographic coordinates (Wartenberg 1985). The method was designed first by Lee (1969) and demonstrated for geological data. Biological relevance was mentioned by Gittins (1979) and documented by Wartenberg (1985). Algorithms underlying the technique are found in Lee (1969) and Wartenberg (1985).

2.5. Examples of the trend surface applications

The following examples elucidate typical trend surface analysis applications in ecological and vegetation work. Information is given about type of data which can be analysed by means of TSA and the main elements of ecological interpretation of the results, including problems that the user should keep in mind.

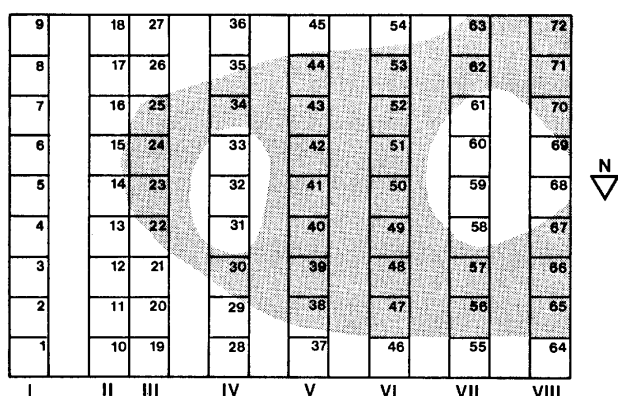


Fig. 1. Sampling design in the Pirin Planina Mts., Bulgaria. Arabic and Roman numerals indicate quadrats and transects respectively. The shaded area is a depression. After Mucina and Poláček (1982).

2.5.1. Single-species pattern

A single-species pattern inferred by TSA will be presented in this section. The data describe a transitional mire in the Pirin Planina Mountains, south-western Bulgaria, at a location near Lake Muratovo Ezero (for further particulars on the site see Mucina and Poláček 1982). In the transitional mire 8 parallel belt transects, each 0.3 m in width, and placed at 0.3 m intervals (except for the transects II and III, Fig. 1), were laid. Each transect was divided into 9 plots (0.3 to 0.3 m each), and plant species cover values were estimated using the Londo (1976) decimal scale. The values were transformed according to Londo's method.

Nardus stricta was chosen for the TSA pattern inference (Figs. 2a-e). The trend (degree 1) shown is a typical linear pattern of isolines. The abundance of *Nardus stricta* increases from NW to SE. The linear function depicts 22% of the total variation in data (Tab. 1). Higher degree trends achieve better fit. Trend degree 5 accounts for 62% of the variation. With the increase of degree the computed trend function values also increase compared to the those measured in the field. At the same time, the TSA pattern becomes more complicated and number of polynomial coefficients increases accordingly. The trend degrees 1, 2, 3, 4 and 5 are represented respectively by 3, 6, 10, 15 and 21 polynomial coefficients. However, the high-order polynomials are known for their instability (Goodman 1983a, Unwin 1975), and therefore only low-degree trends are suggested for interpretations. Goodman (1983a) suggested to use trend degree 3, but our study has shown (Mucina and Poláček 1982) that some high-order degrees might be of importance and meaningful from the viewpoint of ecological interpretation.

A comparison of the D (goodness of fit) values in Tab. 1 shows that the particular trend degree does not contribute proportionally to the variance explained in

Tab. 1. Coefficients of trend functions for *Nardus stricta*. See explanations in the main text.

Trend degree	5	4	3	2	1
B (U)	6.53	6.67	8.97	7.96	5.89
B (1) U	9.73	7.01	-1.55	-1.98	-0.83
B (2) V	-7.20	-12.36	-11.47	-4.77	-0.94
B (3) U V	-13.22	-11.04	0.66	0.10	
B (4) U ²	7.72	-7.35	-0.19	0.26	
B (5) V ²	18.19	23.66	8.26	1.51	
B (6) U ² V	1.63	2.82	-2.19		
B (7) U V ²	16.53	6.21	-0.20		
B (8) U ³	-8.53	2.52	8.17		
B (9) V ³	-22.18	-15.75	-1.77		
B (10) U ³ V	-0.36	-0.18			
B (11) U ² V ²	0.97	-0.75			
B (12) U V ³	-10.48	-0.97			
B (13) U ⁴	3.01	-0.29			
B (14) V ⁴	11.59	3.29			
B (15) U ⁴ V	2.80				
B (16) U ⁴ V ²	-1.63				
B (17) U ² V ³	-0.45				
B (18) U V ⁴	2.35				
B (19) U ⁵	-0.34				
B (20) V ⁵	-2.12				
F-value	4.21	4.69	4.22	6.41	9.89
D-value	0.62	0.54	0.38	0.33	0.22

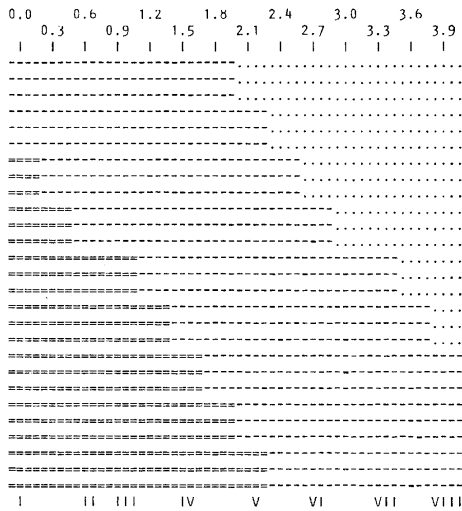
the data. A statistical test might be adopted to decide whether an explanatory contribution of a trend degree is significant or not, and which trend degree should be taken as the terminal one (Poláček 1982). In our case, we used degree 5 as the terminal value. The TSA map of the latter trend shows *Nardus stricta* to be mapped in elevated habitats with high cover values, while low values are indicated in the depressions.

The pattern of *Juncus filiformis* on the same site (Mucina and Poláček 1982) was shown to be complementary to that of *Nardus stricta* (Fig. 3). Comparisons of the TSA patterns of *Nardus stricta* and *Juncus filiformis* with the original values revealed some discrepancies. One is a high theoretical value in locations where no specimens of the species were recorded. There are at least two possible explanations for this discrepancy. Firstly, it can be ascribed to the smoothing effect of the trend function, in another words, all theoretical values depend upon all the others. Secondly, this might be a corollary of an edge effect if the discrepancy occurs on the edge of the studied area (Unwin 1975). A buffer region which includes some plots outside the study area is suggested to complement the analysis (Davis 1973).

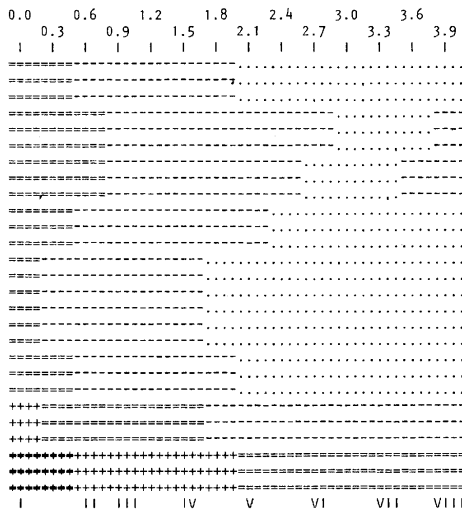
2.5.2. Multi-species pattern

The TSA inference of a multi-species pattern will be shown on the same data set as in the previous exam-

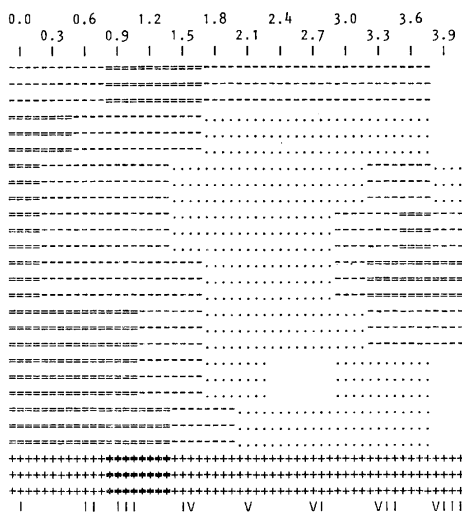
Nardus stricta - trend degree 1



Nardus stricta - trend degree 3



Nardus stricta - trend degree 5



Scale: ---- === ++++ *****
 < 0 0≤2 2≤4 4≤6 6≤8 8>

coordinates

--- 2.4 (9)

--- 2.1 (8)

--- 1.8 (7)

--- 1.5 (6)

--- 1.2 (5)

--- 0.9 (4)

--- 0.6 (3)

--- 0.3 (2)

--- 0.0 (1)

transects

coordinates

--- 2.4 (9)

--- 2.1 (8)

--- 1.8 (7)

--- 1.5 (6)

--- 1.2 (5)

--- 0.9 (4)

--- 0.6 (3)

--- 0.3 (2)

--- 0.0 (1)

transects

coordinates

--- 2.4 (9)

--- 2.1 (8)

--- 1.8 (7)

--- 1.5 (6)

--- 1.2 (5)

--- 0.9 (4)

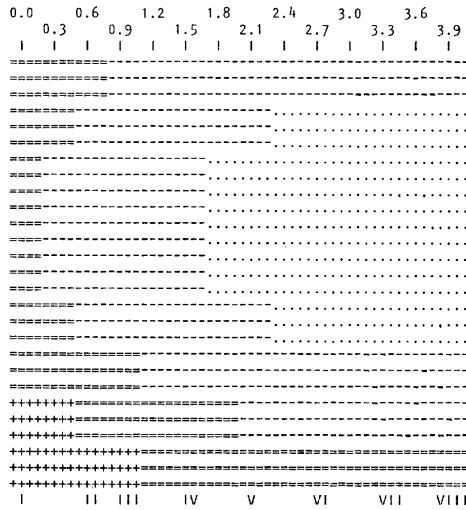
--- 0.6 (3)

--- 0.3 (2)

--- 0.0 (1)

transects

Nardus stricta - trend degree 2



Nardus stricta - trend degree 4

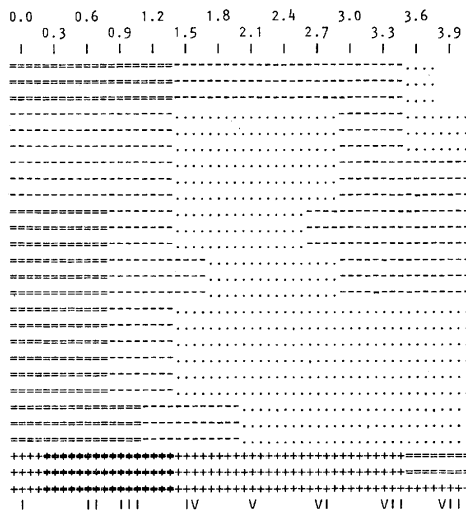


Fig. 2. TSA patterns for *Nardus stricta* in the transition mire site (see Fig. 1) for trend degrees 1 through 5 (a through e).

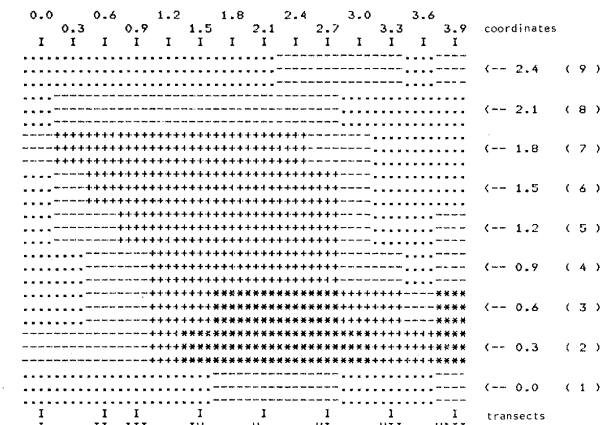


Fig. 3. TSA patterns for *Juncus filiformis* in the transitional mire site (see Fig. 1).

ple. In this particular case, the original data matrix (19 taxa and 72 plots) was submitted to a principal components analysis (PCA, for explanation see Orlóci 1978) and varimax rotation of the PCA axis was performed (Kaiser 1958, see Mucina and Poláček 1982). The obtained PCA scores of plots were used as dependant variables in TSA.

Three vegetation types were distinguished on the studied site: the *Nardus stricta*-*Polytrichum alpinum* type, *Carex fusca*-*Campylopus chrysophyllum* type and

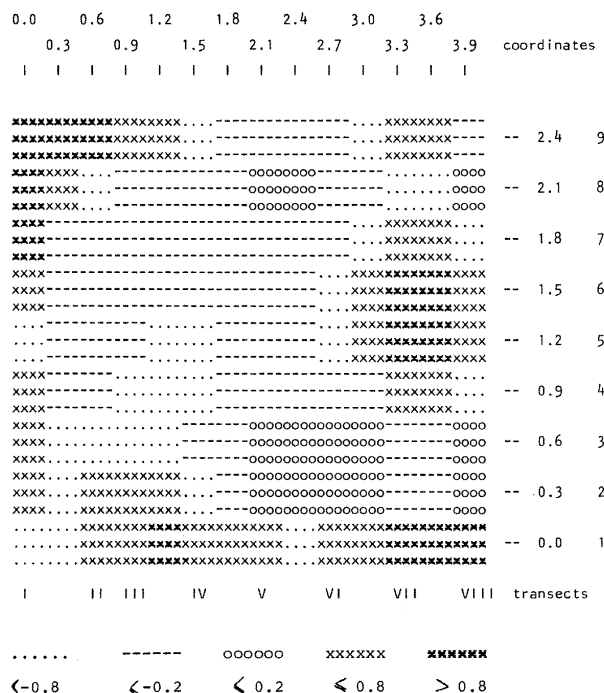


Fig. 4. TSA pattern for PCA scores on axis 1 associated with the *Nardus stricta* group. After Mucina and Poláček (1982).

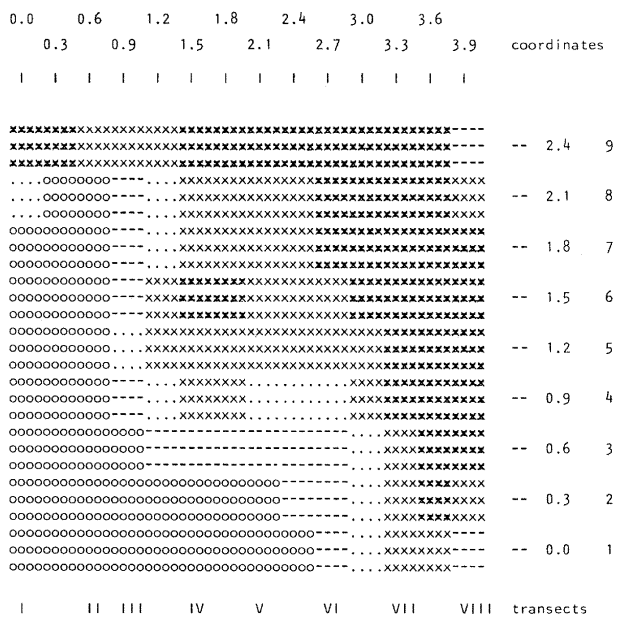


Fig. 5. TSA pattern for PCA scores on axis 2 associated with the *Juncus filiformis* group. After Mucina and Poláček (1982).

Juncus filiformis-*Aulacomium palustre* type. These were characterized by three species groups, including the *Nardus stricta* group, *Juncus filiformis* group, and *Carex nigra* group that characterized PCA axes 1, 2, 3. When the PCA scores of sample plots belonging to the 3 vegetation types were analysed by TSA, three vegetation patterns could be detected. The TSA analysis of the scores for axis 1 detected the spatial (surface) pattern of the *Nardus stricta* group. It is shown (Fig. 4) that this group is mapped in dry elevated habitats, in the E part of the studied area, while the *Carex nigra* group (Fig. 5) is mapped in elevated habitats (hummocks and on borders of depressions) in the W part of the area. The *Juncus filiformis* group (Fig. 6) is mapped in depressions. A close inspection of the patterns of the *Nardus stricta* and *Juncus filiformis* groups reveals an interesting fact: there are high theoretical values mapped in the plot #9, transect I, both for axes 1 and 2. This plot is considered an outlier in the PCA ordination on both axis 1 and 2, and therefore the high values in the plot are considered an artifact (Fig. 6). This matter points up the need for a careful interpretation of data before entering TSA. The removal of data outliers may be beneficial, such as plot #9 in the example. After its removal, the goodness of fit increased from 8.89% to 9.76%. The increase was from 17.9 to 20.6% for trend degrees 1 and 2.

The presence of an aberrant sample is in fact indicated by the analysis of TSA residua is namely that a for plot #9 in the TSA of degree 5 for the scores on PCA axis 2. Very high or very low residuals are ecologically

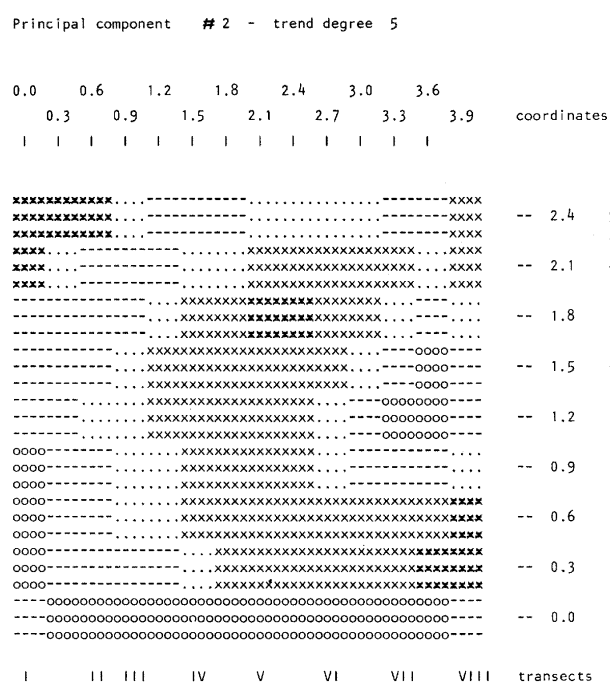


Fig. 6. TSA pattern for the PCA scores on axis 3 associated with the *Carex nigra* group. After Mucina and Poláček (1982).

interpreted as being attributable to strong local factor influences which distort and blur pattern in the data. The local factors were responsible for the high residual in *Carex stellulata* which dominate within plot #9 and causes the outlying position of the plot on the PCA axes (Mucina and Poláček 1982).

2.5.3. Comparison of the trend surface patterns

The data set used to illustrate the comparison of TSA patterns comes from a microzonation system sampled at bare bottom of a sludge pond near Dunajská Streda, western Slovakia (Mucina and Zaliberová 1984).

Four east-west transects perpendicular to the observed zonation system were laid down at the study site. The distance separating the transects is 3 m. 8 rectangular 0.25 m² plots were placed at 2 m distance along the transects to make a quasi-regular grid. Plants of particular species (juvenile and adult well-grown and fertile specimens) were counted separately. In each plot soil samples were taken for estimation of soil-moisture capacity (in %).

Two variables, density of adult specimens of *Persicaria lapathifolia*, and soil moisture values in the sampled plots were selected on purpose as these variables were supposed to produce patterns (Fig. 7).

Tab. 2. Comparison statistics (see Goodman, 1983a, b and section 2.4. in this paper) for TSA images for soil moisture and *Persicaria lapathifolia* in the sludge-pond site.

Trend degree	1°	2°	3°
variation accounted for (soil moisture) %	31.26	37.80	63.60
variation accounted for (<i>Persicaria lapathifolia</i>) %	5.72	23.61	47.40
structural coefficient	−0.787	−0.686	−0.811
distortion between standardized surfaces	3.1937	3.8105	5.8510
unweighted taxonomic distance between coefficients	0.353	1.311	1.912
weighted taxonomic distance between coefficients	4.351	3.060	2.960
correlation between coefficients (weighted situation)	not defined	−0.853	−0.752
correlation between coefficients (unweighted situation)	not defined	−0.917	−0.974
product-moment correlation coefficient	not defined	0.725	0.924
correlation of raw data	−0.465	strike of linear surface (<i>Persicaria lapathifolia</i>)	199.47
strike of linear surface (soil moisture)	0.000	cosine of angular difference	−0.9428

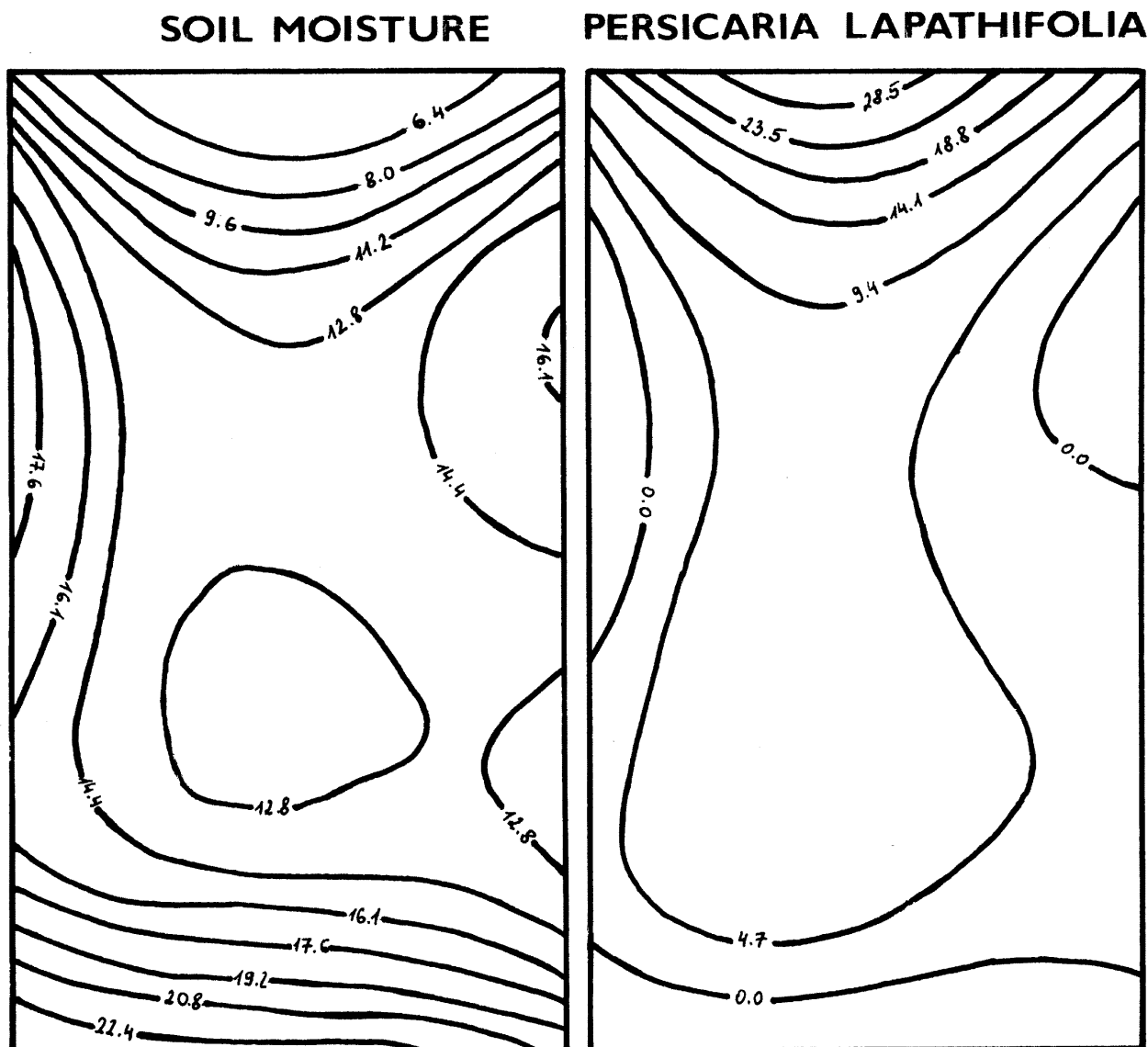


Fig. 7. TSA patterns for soil moisture and *Persicaria lapathifolia* in the sludge-pond site (after Mucina and Zaliberová 1984). Contours correspond to theoretical values computed by the polynomial TSA algorithm incorporated in the COMPARE programme of Goodman (1983a).

Persicaria lapathifolia is most abundant in drained habitats (Mucina and Zaliberová 1984).

Already the product-moment correlation of raw data shows negative relationship. This becomes more pronounced in the structural correlation. This, for the 3rd order (-0.811 , see Tab. 2), indicates mirroring behaviour of variables over the studied area. Also the correlations computed between the trend surface coefficients (both for 2nd and 3rd order) show very high negative values. The third facet of the TSA comparisons, the correlation of surface orientation (see section 2.3) points to varying orientation as the cos angular difference (Tab. 2) attains a value of -0.9428 .

It can be hypothesized that the pattern of *Persicaria lapathifolia* and soil moisture is negative over the same plot with regard to point correlation, the correla-

tion of the TSA polynomial coefficients, as well as surface morphology (defined as surface orientation). As pointed out by Goodman (1983a), an inference of relations between the fitted variables must be done with caution, especially in cases of a low goodness of fit. This, however, was not our case, since for the 3rd order polynomial surface the fit of *Persicaria lapathifolia* and soil moisture were 47.4 and 63.6% respectively.

2.6 Current programmes for TSA

A number of trend surface analysis programmes are available from the Kansas State Geological Survey (Harbaugh 1963, Good 1964, O'Leary *et al.* 1966, Sampson and Davis 1966, Cole *et al.* 1967). These programmes are written in Fortran II, Fortran IV and

Balgol. Clark (1977) published a programme for four-dimensional TSA and Campbell (1974) for stepwise TSA (see also Casetti and Semple 1968). Recent programme in Fortran IV for comparison of TSA imageries (see the section 2.3) is described by Goodman (1983a). Canonical trend surface analysis can be computed by the Fortran IV programme of Lee (1969), which is available through the Kansas State Geological Survey.

3. Splines

3.1. Introduction

In representation of ecological data by means of visualization methods the usual lack of sufficient amount of data prevents the representation of the measured phenomenon in terms of smooth surfaces. This is one of the reasons why a good interpolation method at hand is welcome. Most often the interpolation methods are based on high-order polynomials. The input data are supposed to be ordered in a rectangular regular grid or in a topologically analogous (equivalent) regular grid. The methods of polynomial interpolations allow handling of data which show irregular distribution pattern on the grid. The irregularly patterned data can be, however, transformed on a regular grid by interpolation that is also termed regularization.

The field of interpolation methods experienced great advances during the last decade. This particularly holds true for methods handling irregularly patterned data. First, we review spline methods designed for data distributed on rectangular regular grids, and secondly, the methods for interpolation on irregular grids. Only basic elements of the theory and methods will be presented. Readers interested in more detail are referred to literature sources listed in the References. A software overview on spline techniques and algorithms is also presented.

3.2. Bicubic spline interpolation

Let us suppose that measured data are distributed on a rectangular grid defined as a sets of points

$$X = (x_0, x_1, x_2, \dots, x_M) \quad (20)$$

and

$$Y = (y_0, y_1, y_2, \dots, y_N) \quad (21)$$

where

$$x_{i-1} < x_i \quad \text{for } \forall i = 1, \dots, M$$

and

$$y_{j-1} < y_j \quad \text{for } \forall j = 1, \dots, N.$$

For any cell in the rectangular grid

$$R_{ij} = \{x_{i-1} < x < x_i, y_{j-1} < y < y_j\} \quad (22)$$

and a bicubic polynomial is defined as follows:

$$P_{ij}(x, y) = \sum_{k=0}^3 \sum_{l=0}^3 C_{kl} (x - x_{i-1})^k (y - y_{j-1})^l \quad (23)$$

where $(x, y) \in R_{ij}$.

It should be stressed that the points forming the rectangular grid need not necessarily be equidistant.

For a two-dimensional grid formed by sets of points X and Y , symbolised as Π , the function $s_{\Pi}(x, y)$ is called a bicubic spline under conditions that

(1) in any rectangle $R_{i,j}$ it has a form of the polynomial (Eq. 22),

(2) it has continuous partial second derivatives.

De Boor (1962) defined the polynomial coefficients on the basis of partial derivatives computed by solving triangular systems of linear equations.

Local spline interpolation (Akima 1970, 1972, 1974a, b) is sufficient in most applications. The partial derivatives are approximated by local schemes. The local character of splines is advantageous in designed programmes for graphical presentation on mini- and microcomputers.

The matrix of coefficients is computed by multiplication of matrices:

$$A(\Delta x) * B A^T(\Delta y) = C, \quad \text{where} \quad (24)$$

$$A(h) = \begin{bmatrix} 1 & 0 & 0 & 0 \\ 0 & 1 & 0 & 0 \\ -3/h^2 & -2/h^2 & -3/h^2 & -1/h^2 \\ 2/h^3 & 1/h^2 & 2/h^3 & 1/h^2 \end{bmatrix} \quad (25)$$

$$B(f) = \begin{bmatrix} f_{i-1,j-1} & f_{y_{i-1,j-1}} \\ f_{x_{i-1,j-1}} & f_{xy_{i-1,j-1}} \\ f_{i,j-1} & f_{y_{i,j-1}} \\ f_{x_{i,j-1}} & f_{xy_{i,j-1}} \end{bmatrix} \quad (26)$$

$$\begin{bmatrix} f_{i-1,j} & f_{y_{i-1,j}} \\ f_{x_{i-1,j}} & f_{xy_{i-1,j}} \\ f_{i,j} & f_{y_{i,j}} \\ f_{x_{i,j}} & f_{xy_{i,j}} \end{bmatrix}$$

$$\text{and} \quad \begin{aligned} \Delta x &= x_i - x_{i-1}, \\ \Delta y &= y_j - y_{j-1}, \end{aligned}$$

$$f_x = \frac{\delta f}{\delta x}, \quad f_y = \frac{\delta f}{\delta y} \quad \text{and} \quad f_{xy} = \frac{\delta f}{\delta x \delta y}.$$

The theoretical basis for the derivation of Eqs. 22 and

24 is discussed in de Boor (1962, 1978). Analogous schemes for parametric bicubic splines can be derived for regular grids, which are topologically equivalent to the rectangular regular grids (Fergusson 1964, Hessing *et al.* 1972). According to the latter authors a grid is considered topologically equivalent (Fig. 8) when it can be decomposed into subsets V_0, \dots, V_M and H_0, \dots, H_N to meet the following conditions:

- (1) point $A \in V_k$ and $B \in V_{k+1}$ then $x_A < x_B$,
- (2) the angle of straight line crossing $A, B \in V_k$ with the axis y is less than 45° ,
- (3) $V_k \neq \phi$ (empty set),
- (4) the boundary points are situated on convex hull of the given set.

Analogous conditions must apply also for Hessing *et al.* (1964) brought formulas for local estimates of partial derivatives needed for computing the coefficients of parametric bicubic spline polynomials.

3.3. Interpolation polynomials for irregularly-spaced data

Irregularly spaced data on a surface are most common in the measured data (x_i, y_i, z_i) , $i=1, \dots, p$. Symbols (x_i, y_i) are coordinates in a plane and z_i is a measured value in (x_i, y_i) . The initial algorithms designed for these data are based on least-square methods (Shepard 1968, McLain 1974). Their implementation on computers needed immense numbers of arithmetic operations. The construction of isoline maps is an example. This disadvantages was removed by the method of Akima (1978a, b) which similar to the earlier a method by the same author (1970, 1972, 1974a, b), are based on local approximation of partial derivatives. The relevant algorithm consists of three steps:

- (1) construction of triangular grid;
- (2) estimation of partial derivatives; and
- (3) computation of polynomial coefficients for any triangle of the grid.

The interpolation polynomial is computed as follows:

$$P(x, y) = \sum_{i=0}^5 \sum_{j=0}^{5-i} c_{ji} x^i y^j \quad (27)$$

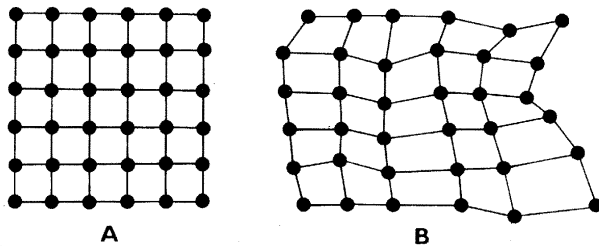


Fig. 8. Two analogous regular grids. A - rectangular equidistant grid, B - non-rectangular grid.

This is a polynomial of the 5th degree, and it is defined by 21 coefficients. Estimation of the partial derivatives (f_x, f_y, f_{xx}, f_{yy} and f_{xy}) is done in 3 vertices of a triangle, which, together with the function (measured) values offer 18 conditions for computing polynomial coefficients for each triangle. The remaining 3 conditions are estimated from normal derivatives in the central points on the triangle edges. The accuracy of the approximations of the derivatives can be affected by selection of a number of neighbouring points (vertices) which are used for their estimation. A triangular grid is defined as a set of points (vertices) irregularly spaced in a plane, which covers the convex hull of the given set of points and meets two criteria:

- (1) the set of vertices of triangles in a grid is identical with the set of measured data points; and
- (2) a common point of two triangles is either a vertex, edge or it is an empty set.

It is obvious that many triangular grids can be constructed for a given set of measured data points. The number of triangles as well as edges is, however, the same for each triangle grid which satisfies the above conditions. The algorithm of Akima (1978a, b) maximizes the minimal angle of a triangle while constructing the triangular grid (step 1). More particulars on this problems are found in Barnhill (1977, 1983), Nielson and Franke (1983), Lawson (1977), and Renka and Cline (1984).

Let us define an interpolant (Shepard 1968) as

$$P(x, y) = \frac{\sum_{i=1}^p d_i^\mu z_i}{\sum_{i=1}^p d_i^\mu}, \quad \text{when } (x, y) \neq (x_i, y_i) \quad (28)$$

$$P(x, y) = Z_i, \quad \text{when } (x, y) = (x_i, y_i) \quad (29)$$

where $d_i = \sqrt{(x - x_i)^2 + (y - y_i)^2}$, p is the number of measured points, z_i is a value in a measured point, and μ is a constant. The interpolant uses all input data points for the computation of the functional value of $P(x, y)$, and its properties are dependent on the choice of the parameter μ (Barnhill *et al.* 1983, Gordon and Wixom 1978). In a modified form, found in Maude (1973), for each point (x_i, y_i) five different points are chosen, and the coefficients of quadratic polynomial Q_i are computed for these chosen points. The polynomial Q_i is then used for the definition of the interpolation polynomial

$$P(x, y) = \frac{\sum_{i=1}^5 w_i Q_i(x, y)}{\sum_{i=1}^5 w_i} \quad (30)$$

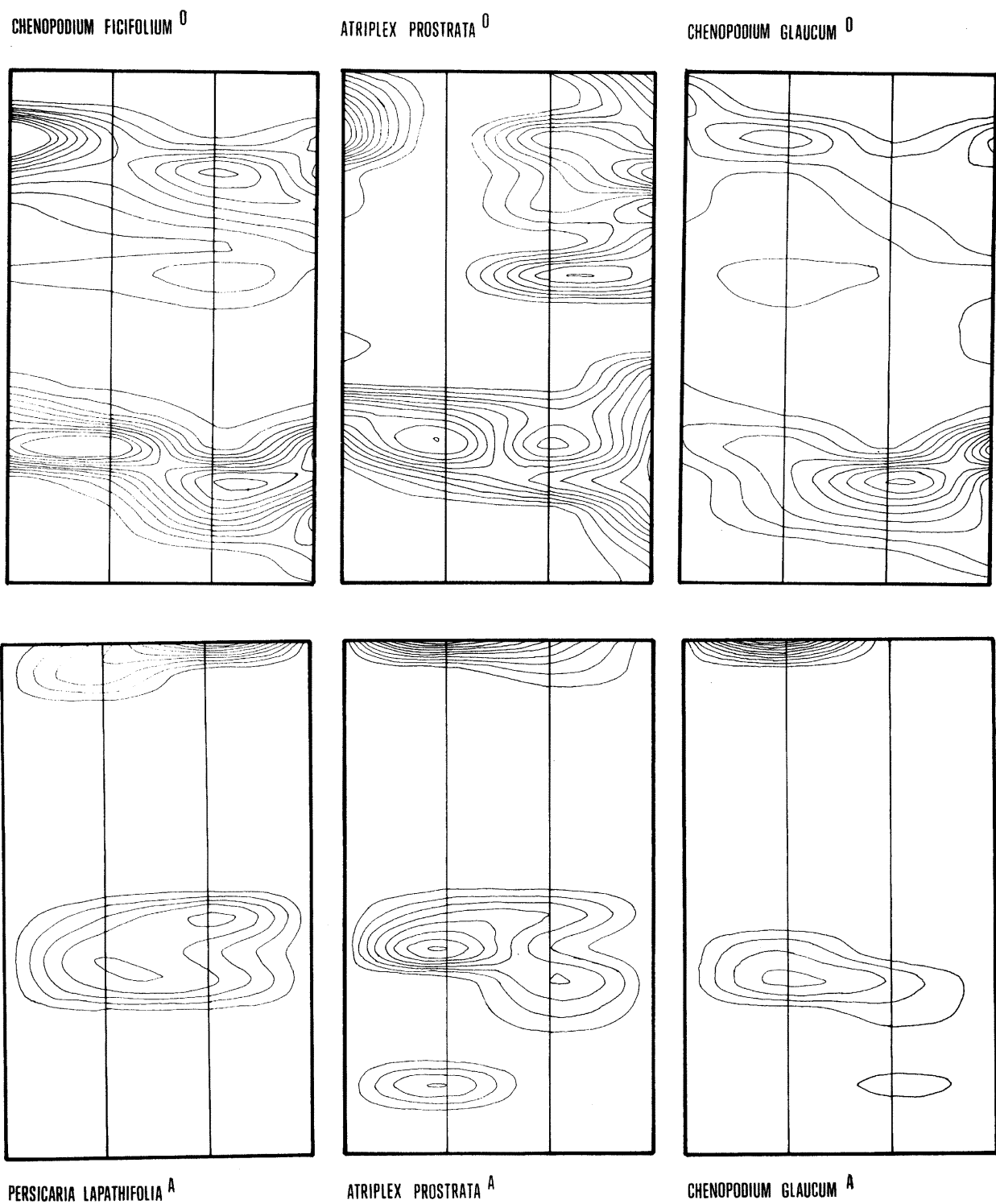
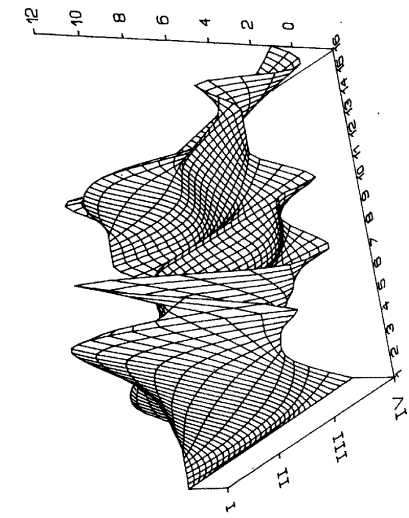
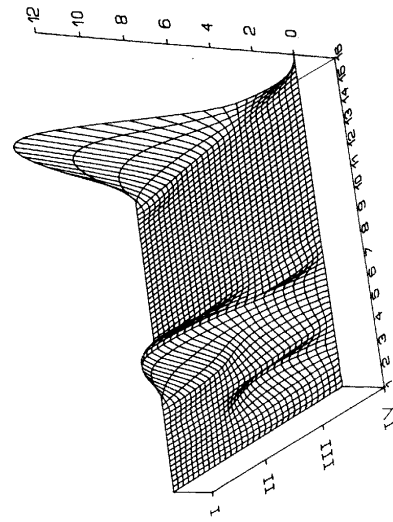


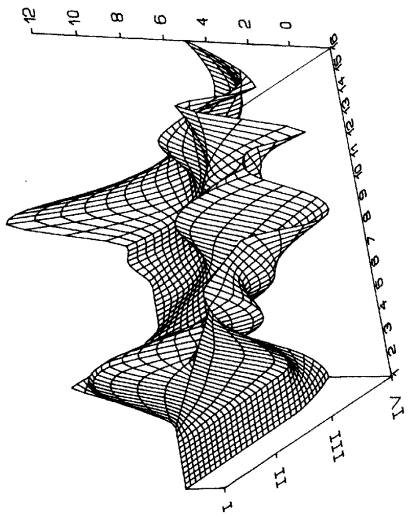
Fig. 9. Isoline spline maps according to the bicubic spline method used for selected group of species (see section 3.4). The distance between two isolines is a 1/10 of the difference between the maximal and minimal value scored for particular species. Maxima for species: *Chenopodium ficifolium*⁰ : 967, *Atriplex prostrata*⁰ : 7, *Chenopodium glaucum*⁰ : 8, *Persicaria lapathifolia*^A : 47, *Atriplex prostrata*^A : 6, and *Chenopodium glaucum*^A : 8. Minima are uniformly zero. Symbols in superscripts identify species in the graph.



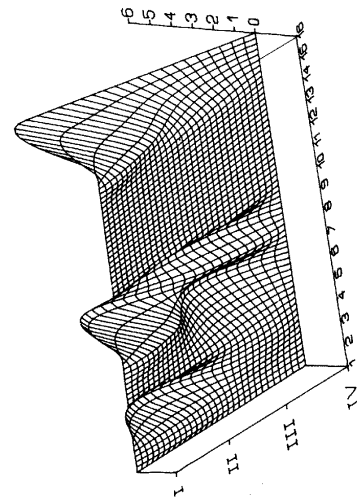
CHENOPODIUM GLAUCUM 0



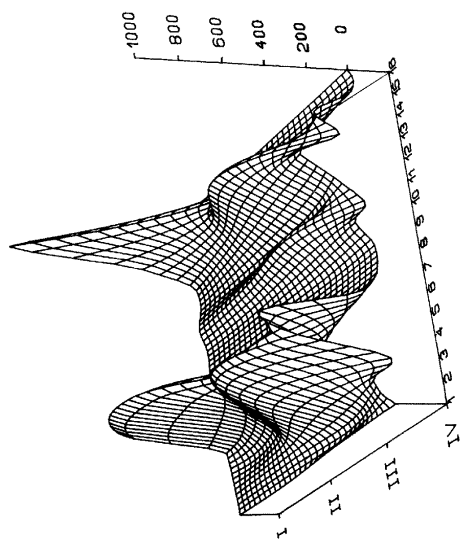
CHENOPODIUM GLAUCUM A



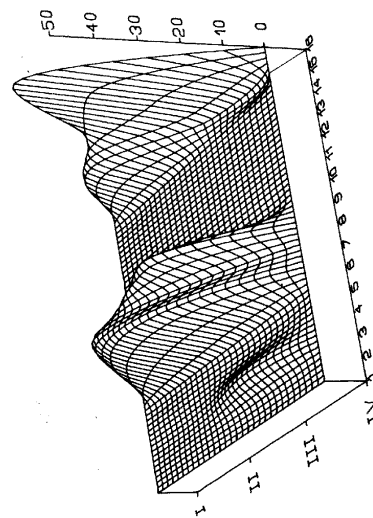
ATRIPLEX PROSTRATA 0



ATRIPLEX PROSTRATA A



CHENOPODIUM FICIFOLIUM 0



PERSICARIA LAPATHIFOLIA A

Fig. 10. Three-dimensional images for spline patterns depicted in Fig. 9. The visualization method is described in the Appendix.

where w_i is a weighting function defined on a circle which contains the point (x_i, y_i) and another group of 5 points. Franke and Nielson (1980) suggested construction of two algorithms based on nodal functions in the form of quadratic polynomials for each point of the grid. These coefficients were used for construction of the interpolation polynomial. In another algorithm, construction of a triangular grid was used by the cited authors. The methods of Maude (1973) and Franke and Nielson (1980) rapidly reduce the number of arithmetic operations.

The interpolation method of Shepard (1968) for irregular patterned data is generalized by Barnhill *et al.* (1983) and Gordon and Wixom (1978) as follows:

$$P(x, y) = \frac{\sum_{i=1}^m [T_m F(x, y)] / d_i^2}{\sum_{i=1}^m 1 / d_i^2} \quad (31)$$

where T_m is a Taylor expansion of the m -degree. Shepard's interpolation method can be used in higher dimensions as well as by interpolations of irregularly spaced data on a sphere. The data in a regular grid can be used for spline approximation of a smooth surface using the method of Dierckx (1977). Other relevant algorithms were published by Barnhill and Little (1984), Barnhill and Stead (1984), McLain (1976), Franke (1982b), Renka and Cline (1984) and Schmidt (1983).

Kriging is another method, differing from those defined by Equations 20 to 31, based on theory of regionalized variables introduced by Matheron (1965, 1967, 1970). It is exact interpolation and allows estimation of error. A modification of the original algorithm was published by McBratney *et al.* (1981). Matheron (1980) and Dubrule (1983) describe comparisons with the spline methods. A comparison of various interpolation methods can be found in Franke (1982a) and a bibliography in Goodman (1985).

3.4. An example of spline application

The data from the experiment in the sludge-pond (see section 2.4.3.) were used for demonstration of spline interpolation over a regular grid. A physiognomically well-distinguished vegetation zonation, consisting of *Echinochloo-Polygonetum* (elevated habitats), *Chenopodietum ficifolii* (low-situated habitats) and a transitional type between the above (Mucina and Zaliberová 1984), was sampled. *Echinochloo-Polygonetum* and *Chenopodietum ficifolii* are associations characterized by two species groups which alternate in the community zones. Local abundance maxima of juvenile specimens of *Chenopodium ficifolium*, *Atriplex prostrata*, and *Chenopodium glaucum* (Figs. 9 and 10) coincide with the location of the zone of *Chenopodietum ficifolii*, a community which is also considered successional young. Adult specimens of *Per-*

sicaria lapathifolia, *Atriplex prostrata*, and *Chenopodium glaucum* characterize the stands of the *Echinochloo-Polygonetum*. As seen from the comparison of the spline images (Figs. 9 and 10), the alternative patterns of the two groups of species are obvious both on isoline and visualized maps.

Applications of splines to mapping of biological data are scarce. Piazza *et al.* (1981) used modified Shepard's splines for mapping gene frequencies in Europe. Bicubic splines were used by Mucina *et al.* (1981) in mapping and comparison of microscale patterns for soil properties and several plant species densities in order to establish possible links between the variables. Eliáš (1984) used the same method for mapping of two oak species over a small area in a oak-hornbeam wood in western Slovakia.

3.5. Current programmes for spline analysis

General problems of interpolation and the mathematical foundation of the spline methodology are summarized by de Boor (1978), including a number of FORTRAN 77 programmes. Basic information on software is provided by Rice (1983), International Software Database (1984), and Siegel (1985).

Specialized computer programme packages were developed by the Association for Computer Machinery (ACM) and International Mathematical Software Library (IMSL). These, for instance, include the Piecewise Polynomial and Spline Routines and the B-Spline Package.

Similar programmes are included in the NaG Library (Numerical Algorithmus Group Ltd., NaG Central Office, Mayfield House, 256 Banbury Rd., Oxford OX27DE, United Kingdom or NaG Inc. 1101 31st Street, Suite 100, Downers Grove, IL 60515, U.S.A.). Other references to published programmes on splines and similar procedures are given by Goodman (1985). Interpolation methods and relevant software are mentioned in the Communications of ACM, Journal of ACM, Computers and Geosciences, The Rocky Mountain Journal of Mathematics (a special volume in 1984) and the Journal of Computer Aided Geometric Design.

Acknowledgement. The authors are grateful to the editors and reviewers for helpful comments and revisions. Kluwer Academic Publishers kindly granted permission to reproduce Figs. 1, 2, 3, 5 and 8.

REFERENCES

- AKIMA, H. 1970. A new method of interpolation and smooth curve fitting based on local procedures. J. ACM 17: 589-602.
- AKIMA, H. 1972. Algorithm 422 - interpolation and smooth curve fitting based on local procedures. Comm. ACM 15: 914-918.
- AKIMA, H. 1974a. Algorithm 474 - bivariate interpolation and smooth surface fitting based on local procedures. Comm. ACM 17: 26-31.
- AKIMA, H. 1974b. A method of bivariate interpolation and smooth surface fitting based on local procedures. Comm.

- ACM 17: 18-20.
- AKIMA, H. 1978a. Algorithm 526 - a method of bivariate interpolation and smooth surface fitting for irregularly distributed data points. *ACM Trans. Math. Software* 4: 160-164.
- AKIMA, H. 1978b. A method of bivariate interpolation and smooth surface fitting for irregularly distributed data points. *ACM Trans. Math. Software* 4: 148-159.
- BARNHILL, R.E. 1977. Representation and approximation of surface. In J.R. Rice (ed.), *Mathematical software*, III., pp. 69-120. Academic Press, N.Y.
- BARNHILL, R.E. 1983. A survey of representation and design of surfaces. *IEEE Comp. Graph. Appl.* 3: 9-16.
- BARNHILL, R.E., DUBE, R.P. and F.F. LITTLE. 1983. Properties of Shepard's surfaces. *Rocky Mountain J. Math.* 13: 365-382.
- BARNHILL, R.E. and F.F. LITTLE. 1984. Three and four-dimensional surfaces. *Rocky Mountain J. Math.* 14: 77-101.
- BARNHILL, R.E. and S.E. STEAD. 1984. Multistage trivariate surfaces. *Rocky Mountain J. Math.* 14: 103-117.
- BONHAM, C.D. 1971. ECOMAP: A computer program for mapping ecological data. *Range Sci. Dept. Sci. Ser.*, Colorado State Univ., 9: 1-30.
- DE BOOR, C. 1962. Bicubic spline interpolation. *J. Math. Phys.* 41: 212-218.
- DE BOOR, C. 1978. *Practical guide to the splines*. Applied Mathematical Series 27. Springer Verlag, N.Y.
- CAMPBELL, R.S. 1974. A generalized stepwise trend surface program - GSTR - I. *Comp. Appl. Nat. Soc. Sci.* 1: 161-170.
- CASETTI, E. and R.K. SEMPLE. 1968. A method for the stepwise separation of spatial trends. *Disc. Pap. 11*, Michigan Inter-Univ. Comm. of Math. Geographers, Ann Arbor.
- CLARK, I. 1977. SNARK - a four-dimensional trend surface computer program. *Comp. Geosci.* 3: 283-308.
- COLE, A.J., C. JORDAN and D.F. MERRIAM. 1967. FORTRAN II program for progressive linear fit of trend surfaces on a quadratic base using an IBM 1620 computer. *Comp. Contrib.* 15, Kansas State Geol. Survey, Lawrence.
- CURTIS, D.J. and E.M. BIGNAL. 1985. Quantitative description of vegetation physiognomy using vertical quadrats. *Vegetatio* 63: 97-104.
- DARGIE, T.C.D. 1984. On the integrated interpretation of indirect site ordinations: a case study using semi-arid vegetation in southeastern Spain. *Vegetatio* 55: 37-55.
- DAVIS, J.C. 1973. *Statistics and data analysis in geology*. J. Wiley and Sons, N.Y.
- DIERCKX, P. 1977. An algorithm for least-squares fitting of cubic spline surfaces to functions on rectilinear mesh over a rectangle. *J. Comp. Appl. Math.* 3: 113-129.
- DUBRULE, O. 1983. Two methods with different objectives: splines and kriging. *J. Int. Ass. Math. Geol.* 15: 245-257.
- DURAZZI, J.T. and F.G. STEHLI. 1972. Average generic age, the planetary temperature gradient, and pole location. *Syst. Zool.* 21: 384-389.
- ELIÁŠ, P. 1984. Horizontal structure of the *Quercus*-species coenopopulations in an oak-hornbeam forest. *Ekológia (ČSSR)*, Bratislava, 3: 399-411.
- FERGUSON, J. 1963. Multivariate curve interpolation. *J. ACM* 11: 221-228.
- FISHER, D.R. 1968. A study of faunal resemblance using numerical taxonomy and factor analysis. *Syst. Zool.* 17: 48-63.
- FRANKE, R.H. 1982a. Scattered data interpolation: tests of some methods. *Math. Comp.* 32: 181-200.
- FRANKE, R.H. 1982b. Smooth interpolation of scattered data by local thin plate splines. *J. Comp. Appl. Math.* 8: 273-281.
- FRANKE, R.H. and G.M. NIELSON. 1980. Smooth interpolation of large sets of scattered data. *IJNME* 15: 1691-1704.
- GITTINS, R. 1968. Trend-surface analysis of ecological data. *J. Ecol.* 56: 845-869.
- GITTINS, R. 1979. Ecological applications of canonical analysis. In: L. ORLÓCI, C.R. RAO and W.M. STITELER (eds.), *Multivariate methods in ecological work*, pp. 309-535. *Stat. Ecol. Serv.*, Vol. 7. ICPH, Fairland, Maryland.
- GOOD, D.I. 1964. Trend surface fitting program for the IBM 1620. *Spec. Distrib. Pap. 14*, Kansas State Geol. Survey, Lawrence.
- GOODMAN, A. 1983a. COMPARE: A FORTRAN IV program for the quantitative comparison of polynomial trend surfaces. *Comp. Geosci.* 9: 417-545.
- GOODMAN, A. 1983b. Data clusters and trend surfaces. *Monash Publ. Geogr.* 29: 1-57.
- GOODMAN, A. 1985. Surface analysis: a structured bibliography. *Dept. Geogr., Monash Univ., Working Pap.* 17: 1-81.
- GORDON, W.J. and J. WIXOM. 1978. On Shepard's method of metric interpolation to bivariate and multivariate data. *Math. Comp.* 32: 253-264.
- GRANT, F. 1957. A problem in the analysis of geophysical data. *Geophysics* 22: 309-344.
- GREEN, P.E., 1978. *Analyzing multivariate data*. The Dryden Press, Hinsdale, IL.
- HAGGET, P., A.D. CLIFF and A. FREY. 1977. *Locational analysis in human geography*. 2nd ed. Vols. 1 and 2. Edward Arnold, London.
- HARBAUGH, J.W. 1963. BALGOL program for trend surface mapping using an IBM 7090 computer. *Spec. Distrib. Pap. 3*, Kansas Geol. Survey, Lawrence.
- HENGVELD, R. 1979. The analysis of spatial patterns of some ground beetles (Col. Carabidae). In: R.M. CORMACK and J.K. ORD (eds.), *Spatial and temporal analysis in ecology*, pp. 333-346. *Stat. Ecol. Ser.*, Vol. 8. ICPH, Fairland, Maryland.
- HESSING, R.C., H.K. LEE, A. PIERCE and E.N. POWERS. 1972. Automatic contouring using bicubic functions. *Geophysics* 37: 669-674.
- HOTELLING, H. 1936. Relations between two sets of variates. *Biometrika* 28: 321-377.
- INTERNATIONAL SOFTWARE DATABASE. 1984. *The software catalog. Microcomputers*. Elsevier, Amsterdam.
- JUMARS, P.A. 1978. Spatial autocorrelation with RUM: Vertical and horizontal structure of a bathyal benthic community. *Deep Sea Res.* 25: 589-604.
- JUMARS, P.A., D. THISTLE and M.L. JONES. 1977. Detecting two-dimensional structure in biological data. *Oecologia* 28: 109-123.
- KAISER, H.F. 1958. The varimax criterion for analysis rotation in factor analysis. *Psychometrika* 23: 187-200.
- KOOLJMAN, S.A.L.M. and R. HENGVELD. 1979. The description of a non-linear relationship between some Carabid beetles and environmental factors. In: G.P. PATIL and M.L. ROSENZWEIG (eds.), *Contemporary quantitative ecology and related econometrics*, pp. 635-647. *Stat. Ecol. Ser.* 12. ICPH, Fairland, Maryland.
- KRUMBEIN, W.C. 1959. Trend surface analysis of contour-type maps with irregular control-point spacing. *J. Geophys. Res.* 64: 823-834.
- KUBERT, B., J. SZABO and S. JULIERI. 1968. The perspective representation of functions of two variables. *J. ACM* 15.

- LAWSON, C.L. 1977. Software for C^1 surface interpolation. In: J.R. RICE (ed.), *Mathematical software*. III., pp. 161-194. Academic Press, N.Y.
- LEE, P.J. 1969. The theory and application of canonical trend surfaces. *J. Geol.* 77: 303-318.
- LONDO, G. 1976. The decimal scale for relevés of permanent plots. *Vegetatio* 33: 61-64.
- MATHERON, G. 1965. *Les variables régionalisées et leur estimation*. Masson, Paris.
- MATHERON, G. 1967. Kriging, or polynomial interpolation procedures? *Can. Min. Metal. Bull.* 60: 1041-1045.
- MATHERON, G. 1970. The theory of regionalized variables and its applications. *Cah. Centre Morphol. Math.*, Paris, 5.
- MATHERON, G. 1980. Splines and kriging: their formal equivalence. *Ecole Nationale Supérieure des Mines de Paris*, pp. 1-20.
- MAUDE, A.D. 1973. Interpolation - mainly for graph plotter. *Comp. J.* 16: 64-65.
- McANDREWS, J.H. and D.M. POWER. 1973. Palynology of the Great Lakes: the surface sediments of Lake Ontario. *Can. J. Earth Sci.* 10: 777-792.
- McBRATNEY, A.B., R. WEBSTER and T.M. BURGESS. 1981. The design of optimal sampling schemes for local estimation and mapping using regionalized variables. I-II. *Comp. Geosci.* 7: 331-365.
- McLAIN, D.H. 1974. Drawing contours from arbitrary data points. *Comp. J.* 17: 318-324.
- McLAIN, D.H. 1976. Two dimensional interpolation from random data. *Comp. J.* 19: 178-181.
- MIRCHINK, M.F. and V.P. BUKHARTSEV. 1954. The possibility of a statistical study of structural correlations. (Russian). *Dokl. Akad. Nauk U.S.S.R.* 126: 1062-1065.
- MORRISON, D.F. 1976. *Multivariate statistical methods*. 2nd ed. McGraw-Hill, N.Y.
- MUCINA, L. and S. POLÁČIK. 1982. Principal components analysis and trend surface analysis of a small-scale pattern in a transition mire. *Vegetatio* 48: 165-173.
- MUCINA, L., P. SLAVKOVSKÝ and V. ČÍK. 1983. Correlations between plant species and environmental factors under real topographical conditions: formulation of hypotheses. (Slovak). *Inst. of Exp. Biol. and Ecol.*, Bratislava.
- MUCINA, L. and M. ZALIBEROVÁ. 1984. A numerical classification approach to vegetation zonation in a sludge pond. *Acta Bot. Slov. Acad. Sci. Slovacae*, Ser. A, Bratislava, Suppl. 1: 239-251.
- NEAL, M.W. and K.A. KERSHAW. 1973. Studies on lichen-dominated systems. IV. The objective analysis of Cape Henrietta Maria raised-beach systems. *Can. J. Bot.* 51: 1177-1190.
- NIELSON, G.M. and R.H. FRANKE. 1983. Surface construction based upon triangles. In: R.E. BARNHILL and W. BOEHM (eds.), *Surface in CAGD*, pp. 163-177. North-Holland, Amsterdam.
- NORCLIFFE, G.B. 1969. On the use and limitations of trend surface models. *Can. Geogr.* 8: 338-348.
- O'LEARY, M., R.M. LIPPERT and O.T. SPITZ. 1966. A FORTRAN IV and MAP program for computation and plotting of trend surface for degrees 1 through 6. *Comp. Contrib.* 3, Kansas State Geol. Survey, Lawrence.
- ORLÓCI, L. 1978. *Multivariate analysis in vegetation research*. 2nd ed. Dr. W. Junk, The Hague.
- PIAZZA, A., P. MENOZZI and L. CAVALLI-SFORZA. 1981. The making and testing of geographic gene-frequency maps. *Biometrics* 37: 635-659.
- POLÁČIK, Š. 1982. Analysis of spatial trends: Study of employment in the main branches of the national economy in Slovakia, 1961 and 1970. (Slovak.) *Stud. Geogr.*, Brno, 74: 143-209.
- READER, R.J. and H. LIETH. 1984. Computer-assisted survey and mapping of vegetation attributes. In: R. KNAPP (ed.), *Sampling methods and taxon analysis in vegetation science*, pp. 171-179. Dr. W. Junk, The Hague.
- RENKA, R.J. and A.K. CLINE. 1984. Triangle-based C^1 interpolation method. *Rocky Mountain J. Math.* 14: 223-237.
- RICE, J.R. 1983. *Numerical methods, software, and analysis*. McGraw-Hill, N.Y.
- ROBINSON, A.H. and L. CAROE. 1967. On the analysis and comparison of statistical surface. In: W.L. GARRISON (ed.), *Quantitative geography. I. Economic and cultural topics*, pp. 252-276. Northwest. Univ. Stud. Geogr.
- SAMPSON, R.J. and J.C. DAVIS. 1966. FORTRAN II trend surface program with unrestricted input for the I.B.M. 1620 computer. *Spec. Distrib. Pap.* 26, Kansas State Geol. Survey, Lawrence.
- SCHMIDT, R.M. 1983. Fitting scattered surface data with large gaps. In: R.E. BARNHILL and W. BOEHM (eds.), *Surface in CAGD*, pp. 185-189. North Holland, Amsterdam.
- SHEPARD, D. 1968. Two dimensional interpolation function for irregularly spaced data. *Proc. 23rd Nat. Conf. ACM*: 517-523.
- SIEGEL, J.B. 1985. *Statistical software for microcomputers*. North-Holland, Amsterdam.
- SNEATH, P.H.A. 1966. Estimating concordance between geographical trends. *Syst. Zool.* 15: 250-252.
- SNEATH, P.H.A. 1967. Trend surface analysis of transformation grids. *J. Zool.* 151: 65-122.
- SNEATH, P.H.A. and R.R. SOKAL. 1973. *Numerical taxonomy*. Freeman and Co., San Francisco.
- SOKAL, R.R. and M.L. OGDEN. 1978. Spatial autocorrelation in biology. *Biol. J. Linn. Soc.* 10: 199-249.
- SOKAL, R.R. and R. RINKEL. 1963. Geographic variation of a late *Pemphigus populi-transversus* in eastern North America. *Univ. Kansas Sci. Bull.* 44: 467-507.
- STEHLI, F.G. 1964. Permian zoogeography and its bearing to climate. In: A.E.M. NAIRN (ed.), *Problems in palaeoclimatology*. pp. 537-549. J. Wiley and Sons, N.Y.
- STEHLI, F.G. 1965. Paleontologic technique for defining ancient ocean currents. *Science* 148: 943-946.
- STEHLI, F.G. and C.E. HELSLEY. 1963. Paleontologic technique for detecting ancient pole positions. *Science* 142: 1057-1059.
- STEHLI, F.G. and J.W. WELLES. 1971. Diversity and age patterns in hermatypic corals. *Syst. Zool.* 20: 115-126.
- UNWIN, D. 1975. An introduction to trend surface analysis. *Concepts and Techniques in Modern Geography* 5: 1-40.
- WARTENBERG, D. 1985. Canonical trend surface analysis: a method for describing geographic patterns. *Syst. Zool.* 34: 259-279.
- WATSON, C.S. 1971. Trend surface analysis. *Math. Geol.* 3: 215-226.

Appendix

Visualization of spline images

The numerical data obtained by measuring values

over some area define a surface which can be graphically represented to give us immediate information about maxima and minima. The surface is observed from some view point in space. By perspective transformation we can bring into view portions of the surface which we wish to inspect. The surface is represented by a rectangular array in xy -plane.

Definition: Let $\{X_i\}$, $i=1, \dots, n$ be a set of points $X_i = (x_i, 0, 0)$ on the spatial x -axis, $x_{i+1} = x_i + h$, $h > 0$, $i=1, \dots, (n-1)$. Let $\{Y_j\}$, $j=1, \dots, m$ be a set of points $Y_j = (0, y_j, 0)$ on the spatial y -axis, $y_{j+1} = y_j + f$, $f > 0$, $j=1, \dots, (m-1)$. The rectangular array $O(n, m)$ is a set $\{A_{i,j}\}$, $i=1, \dots, n$, $j=1, \dots, m$ of points $A_{i,j} = (x_i, y_j, 0)$, which lies in xy -plane (Fig. 11). The transverse edge of rectangular array $O(n, m)$ is each abscissa $A_{i,j} A_{i,j+1}$, $i=1, \dots, n$, $j=1, \dots, m-1$. The lengthwise edge of rectangular array $O(n, m)$ is each abscissa $A_{i,j} A_{i+1,j}$, $i=1, \dots, n-1$, $j=1, \dots, m$. We considered surface γ , which is represented over the rectangular array $O(n, m)$ and γ will be determined by a set $\{S_{i,j}\}$, $i=1, \dots, n$, $j=1, \dots, m$ of points $S_{i,j} = (x_i, y_j, z_{ij})$. z_{ij} are the coordinates of points of surface γ on the z -axis. The rectangular projection of $S_{i,j}$ on the xy -plane is point $A_{i,j}$ of rectangular array $O(n, m)$. The transverse cut of surface γ is the sequence of abscissa $S_{i,1} S_{i,2} S_{i,3} \dots S_{i,m-1} S_{i,m}$, $i=1, \dots, n$. The lengthwise cut of surface γ is the sequence of abscissa $S_{1,j} S_{2,j} S_{3,j} \dots S_{n-1,j} S_{n,j}$, $j=1, \dots, m$. The total surface γ will be represented by n transverse cuts and by m lengthwise cuts of the surface γ . Let $C = (cx, cy, cz)$ be the viewing point of the observer. The following is a test of visibility for each point $S_{i,j}$ on surface γ .

Test of point visibility (Kubert et al. 1968):

(1) Compute all cross points of abscissa $\overline{C'A_{i,j}}$ which is a rectangular projection of abscissa $\overline{CS_{i,j}}$ into the

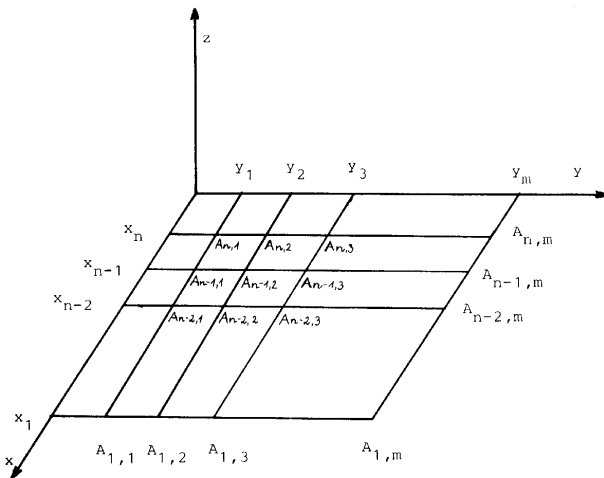


Fig. 11. Rectangular grid $O(n, m)$ composed of points A_{ij} .

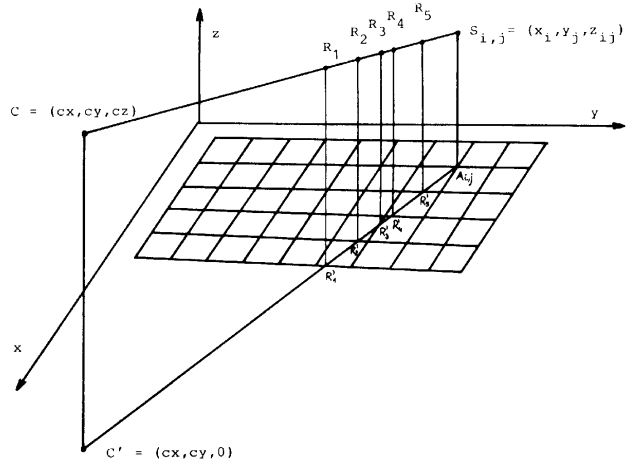


Fig. 12. Cross points R'_i with the rectangular grid $O(n, m)$ and points R_i which lie on the line of view.

xy -plane with all edges of rectangular array $O(n, m)$. We obtain the set $\{R'_i\}$, $i=1, \dots, v$ of cross points R'_i (see Fig. 12).

(2) By the use of linear interpolation we compute z coordinates for points R_k , $k=1, \dots, v$, on the abscissa $\overline{CS_{i,j}}$ and rectangular projections of R_k on the xy -plane R'_k , $k=1, \dots, v$ (Fig. 12). Let $R_k = (rx, ry, rz)$, $R'_k = (rx, ry, 0)$, $C = (cx, cy, cz)$, $S_{i,j} = (x_i, y_j, z_{ij})$. Since R_k lies on the abscissa $\overline{CS_{i,j}}$,

$$\frac{rx-x_i}{cx-x_i} = \frac{ry-y_j}{cy-y_j} = \frac{rz-z_{ij}}{cz-z_{ij}}$$

so that

$$rz = \frac{rx-x_i}{cx-x_i} (cz-z_{ij}) + z_{ij}$$

or

$$rz = \frac{ry-y_j}{cy-y_j} (cz-z_{ij}) + z_{ij}$$

(3) By the use of linear interpolation we compute z coordinates for points T_k , $k=1, \dots, v$, of surface γ , of which the rectangular projections on the xy -plane are point R'_k , $k=1, \dots, v$. Let $A_{i,j} = (x_i, y_j, 0)$, $A_{i,j+1} = (x_i, y_{j+1}, 0)$, $S_{i,j} = (x_i, y_j, z_{ij})$, $S_{i,j+1} = (x_i, y_{j+1}, z_{i,j+1})$, $R'_k = (rx, ry, 0)$, $T_k = (rx, ry, tz)$. Based on these, (Fig. 13).

$$tz = \frac{ry-y_j}{y_{j+1}-y_j} (z_{i,j+1} - z_{ij}) + z_{ij}$$

(4) We determine next the visibility of point $S_{i,j}$ of surface γ from C . We use the differences of the z coordinates of T_k and z coordinates of R_k , $k=1, \dots, s$, on the abscissa of view $\overline{CS_{i,j}}$. Let $R_k = (rx, ry, rz)$ and $T_k = (rx, ry, tz)$. Let $v(R_k, T_k) = tz - rz = v_k$, $\forall k=1, \dots, s$.

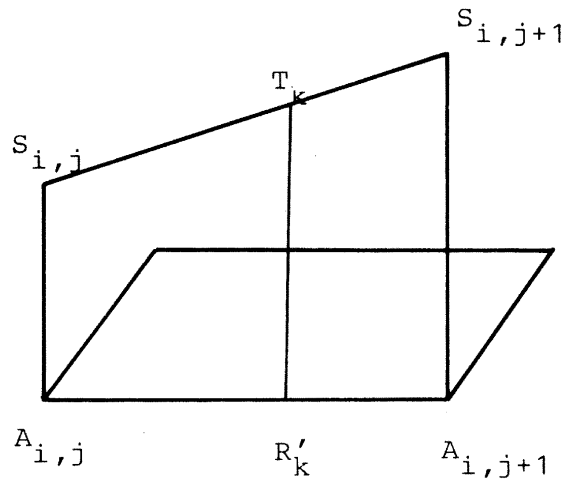


Fig. 13. The point T_k whose rectangular projection on the plane $x-y$ is R'_k . The latter is computed by the linear interpolation method.

If $\forall k=1, \dots, s : v_k > 0$ then point $S_{i,j}$ is visible from below. If $\forall k=1, \dots, s : v_k < 0$ the point $S_{i,j}$ is visible from above. If $\exists t, u ; 1 \leq u, t \leq s : v_k > 0 \wedge v_u < 0$ then point $S_{i,j}$ is hidden.

By the mentioned graphical method we determine first the transverse cut sequences (abscissa),

$$\overline{S_{i,1} S_{i,2}}, \overline{S_{i,2} S_{i,3}}, \dots, \overline{S_{i,m-1} S_{i,m}}, i=1, 2, \dots, n$$

and then we interpret the lengthwise cuts (abscissa),

$$\overline{S_{1,j} S_{2,j}}, \overline{S_{2,j} S_{3,j}}, \dots, \overline{S_{n-1,j} S_{n,j}}, j=1, \dots, m$$

The graphic output was elaborated on the basis of data for the rectangular array 0 (4, 12), i.e., four transverse cuts and twelve lengthwise cuts. This array was refined into another rectangular array 0 (31, 61). By tests we determined that all points above the rectangular array 0 (31, 61) are visible.